NIH Public Access
Author Manuscript
Neuropharmacology. Author manuscript; available in PMC 2014 October 01.

Published in final edited form as:
Neuropharmacology. 2013 October ; 73: 311–319. doi:10.1016/j.neuropharm.2013.05.032.

"P2X7 Receptor Activation Regulates Microglial Cell Death During Oxygen-Glucose Deprivation"

Ukpong B. Eyo[a], **Sam A. Miner**[a], **Katelin E. Ahlers**[a], **Long-Jun Wu**[b], and **Michael E. Dailey**[a]
[a]Department of Biology, University of Iowa, Iowa City, IA 52242

[b]Department of Cell Biology and Neuroscience, Rutgers University, Piscataway, New Jersey 08854

Abstract

Brain-resident microglia may promote tissue repair following stroke but, like other cells, they are vulnerable to ischemia. Here we identify mechanisms involved in microglial ischemic vulnerability. Using time-lapse imaging of cultured BV2 microglia, we show that simulated ischemia (oxygen-glucose deprivation; OGD) induces BV2 microglial cell death. Removal of extracellular Ca^{2+} or application of Brilliant Blue G (BBG), a potent P2X7 receptor (P2X7R) antagonist, protected BV2 microglia from death. To validate and extend these *in vitro* findings, we assessed parenchymal microglia in freshly isolated hippocampal tissue slices from GFP-reporter mice ($CX3CR1^{GFP/+}$). We confirmed that calcium removal or application of apyrase, an ATP-degrading enzyme, abolished OGD-induced microglial cell death *in situ*, consistent with involvement of ionotropic purinergic receptors. Indeed, whole cell recordings identified P2X7R–like currents in tissue microglia, and OGD-induced microglial cell death was inhibited by BBG. These pharmacological results were complemented by studies in tissue slices from P2X7R null mice, in which OGD-induced microglia cell death was reduced by nearly half. Together, these results indicate that stroke-like conditions induce calcium-dependent microglial cell death that is mediated in part by P2X7R. This is the first identification of a purinergic receptor regulating microglial survival in living brain tissues. From a therapeutic standpoint, these findings could help direct novel approaches to enhance microglial survival and function following stroke and other neuropathological conditions.

Keywords

microglia; stroke; P2X7; cell death; ATP; OGD

1. Introduction

Ischemia remains a global health concern, occurring frequently in the elderly as well as in the pre-term and term infant (Nelson, 2007). Research focused on delineating mechanisms of neuronal death and protection has yielded potential targets for therapeutic intervention. Unfortunately, this has not yet translated into successful clinical trials (Ginsberg, 2008).

© 2013 Elsevier Ltd. All rights reserved.

Correspondence: Dr. Michael Dailey, Dept. of Biology, 369 Biology Building, University of Iowa, Iowa City, IA 52242-1324, TEL: (319) 335-1067, FAX: (319) 335-1069, michael-e-dailey@uiowa.edu.

Publisher's Disclaimer: This is a PDF file of an unedited manuscript that has been accepted for publication. As a service to our customers we are providing this early version of the manuscript. The manuscript will undergo copyediting, typesetting, and review of the resulting proof before it is published in its final citable form. Please note that during the production process errors may be discovered which could affect the content, and all legal disclaimers that apply to the journal pertain.

NIH-PA Author Manuscript
NIH-PA Author Manuscript
NIH-PA Author Manuscript

NIH-PA Author Manuscript

NIH-PA Author Manuscript

NIH-PA Author Manuscript

Consequently, glial-based strategies have been proposed to compliment neurocentric approaches (Nedergaard and Dirnagl, 2005; Weinstein et al., 2010; Barreto et al., 2011). However, while the effects of ischemia on astrocytes and oligodendrocytes are being elucidated (Matute et al., 2006; Takano et al., 2009), much less is known about how ischemia affects microglia, the resident immune cells of the CNS.

Debate persists concerning the role of microglia during ischemia. Although some studies suggest that microglia are neurotoxic during ischemia (Yrjanheikki et al., 1998; Wu et al., 2012), there is also considerable evidence for neuroprotective roles for microglia in rodent models of stroke. For example, microglial depletion during ischemia in neonates (Faustino et al., 2011) or adults (Lalancette-Hebert et al., 2007) results in poorer outcomes. Furthermore, introduction of exogenous microglia either before (Hayashi et al., 2006; Kitamura et al., 2004, 2005) or after (Neumann et al., 2006; Imai et al., 2007; Narantuya et al., 2010) experimental stroke reduced neurodamage, suggesting that microglia can promote recovery from stroke. Despite this neuroprotective potential of microglia following stroke, previous studies in *in vitro* cell culture (Lyons and Kettenmann, 1998; Yenari and Giffard, 2001) and acute tissue slices (Eyo and Dailey, 2012) showed that microglia themselves are susceptible to ischemic injury. However, the mechanisms involved in this susceptibility have not been identified.

Studies in astrocytes and oligodendrocytes suggest that calcium dysregulation may contribute to ischemia-induced glial cell death. Metabolic failure in the brain results in extracellular accumulation of neurotransmitters, including glutamate, which activate ionotropic receptors, leading to abnormally high calcium influx. High cytosolic calcium levels, in turn, activate proteases and initiate cell demise (Alberdi et al., 2005; Matute et al., 2006; Szydlowska and Tymianski, 2010). However, it is unknown whether calcium dysregulation mediates ischemia-induced death of microglia, which in the ‘resting’ or ‘surveillant’ state may lack receptors for classical neurotransmitters.

Receptors for non-classical neurotransmitters, including adenosine triphosphate (ATP), are expressed by microglia and may contribute to ischemic cytotoxicity. In addition to its well-known role as an *intracellular* energy source, ATP also functions as an *extracellular* signaling molecule by activating membrane bound receptors including ionotropic P2X receptors and G-protein coupled metabotropic P2Y receptors (Burnstock, 2007). During ischemia, ATP outflow from cells increases *in vivo* (Melani et al., 2005, 2012), in *vivo* brain slices (Frenguelli et al., 2007), and in *in vitro* cell culture (Liu et al., 2008; Domercq et al., 2010). Because high levels of extracellular ATP may activate P2X7 receptors (P2X7Rs), leading to calcium influx and cytotoxicity (Skaper, 2011), they are a candidate for mediating microglial cell death during ischemia. Indeed, P2X7Rs are predominantly expressed by immune cells, and several studies have shown that high levels of ATP induce macrophage and microglial cell death in dissociated cell cultures (Ferrari et al., 1997, 1999; Hanley et al., 2012) and in living tissues (Ryu et al., 2002; Jeong et al., 2010). Therefore, we tested the hypothesis that P2X7R signaling during oxygen and glucose deprivation (OGD), a model for ischemia, is detrimental to microglial survival.

2. Materials and Methods

2.1. BV2 Cell Culture, Imaging, and Cell Death Analysis

BV2 cells were maintained in tissue culture dishes in high glucose Dulbecco’s Modified Eagle’s Medium (DMEM; Gibco) supplemented with 10% heat-inactivated Fetal Bovine Serum (FBS; HyClone), 100 U/mL penicillin, and 100 μg/mL streptomycin (Gibco) in a 37°C CO_2 incubator. BV2 cells were imaged within 12 to 72 hours of plating by modified Hoffman modulation contrast on a Leica DM-IL inverted microscope with stage heating.

NIH-PA Author Manuscript

NIH-PA Author Manuscript

NIH-PA Author Manuscript

Images were captured every 3 min using a 20X/0.7 objective lens. Cell death was determined in time-lapse movies by a sudden change in cell morphology (blebbing or crenulation) followed by absence of cell movement for the duration of imaging. Cell death was further confirmed by labeling with Sytox (1:10,000; Invitrogen) at the end of time-lapse sequences (n = 24 cells; 3 sequences).

2.2. Animals and Preparation of Tissue Slices

For all tissue slice experiments, we used both male and female heterozygous GFP reporter mice ($CX3CR1^{GFP/+}$) expressing GFP under control of the fractalkine receptor (CX3CR1) promoter (Jung et al., 2000; Jackson Labs). For some experiments, P2X7-null mice (Solle et al., 2007; Jackson Labs) were crossed with GFP-expressing mice to produce $P2X7^{-/+}$:$CX3CR1^{GFP/+}$ and $P2X7^{-/-}$:$CX3CR1^{GFP/+}$ siblings. Animals were used in accordance with institutional guidelines, as approved by the animal care and use committee. All efforts were made to minimize animal suffering, to reduce the number of animals used, and to utilize cell culture and *ex vivo* tissue slice alternatives to *in vivo* techniques.

Acutely isolated hippocampal slices were prepared from neonatal (P4-P7) mice as detailed previously (Eyo and Dailey, 2012). Briefly, mice were swiftly decapitated, and brains were removed and placed in ice-cold artificial cerebrospinal fluid (ACSF) with the following composition (in mM): NaCl 124; KCl 3; NaH_2PO_4 1.3; $MgCl_2$ 3; HEPES 10; $CaCl_2$ 3; glucose 10. Excised hippocampi were cut transversely (400 μm thick) using a manual tissue chopper (Stoelting). Slices were maintained in HEPES-buffered ACSF.

2.3. Oxygen-Glucose Deprivation (OGD)

OGD was performed as described previously (Eyo and Dailey, 2012). Briefly, OGD medium was prepared by replacing glucose with sucrose in the ACSF, then 5 mL of ACSF was bubbled with N_2 for 15 minutes. In all tissue slice experiments, either Sytox Orange (Molecular Probes, #S11368) or Topro-3 (Molecular Probes, #T3605) was added to ACSF at 1:10,000 (DMSO concentration at 0.0001%) before N_2 bubbling. The media was warmed briefly in a 37°C water bath and immediately applied to previously mounted slices, and the chamber was sealed and prepared for imaging.

2.4. Time-Lapse Confocal Imaging in Hippocampal Slices

Confocal time-lapse imaging in tissue slices was performed on a Leica SP5 MP confocal/multiphoton imaging system with a *xyz* motorized stage on an upright platform, as described previously (Eyo and Dailey, 2012). Images were taken with a 20X/0.7 Plan Apo objective lens at a resolution of 1.4 pixels/μm. Stacks of 15 confocal images taken 3 μm apart were collected at 10 minute intervals. Image stacks included the surface of the slice to control for any migration of microglia to the slice surface. Image stacks were collected every 10 minutes in order to capture all cell death events (concomitant loss of GFP and gain of Sytox) and to clearly distinguish them from phagocytic uptake of neighboring dead cell nuclei. Multisite imaging enabled concurrent imaging of up to 8 slices with different genotypes (e.g., P2X7Het and P2X7KO). Imaging sessions typically commenced about 20–30 min after tissue slicing and lasted several hours. Illumination and image capturing parameters were set such that there was no appreciable photobleaching of the GFP signal in any of the time-lapse imaging experiments, either during control or experimental conditions.

Drugs were added to glucose-free ACSF prior to N_2 bubbling and were applied to slices throughout imaging. Apyrase (Sigma-Aldrich, no. A6132), a potato enzyme that has both adenosine 5'-diphosphatase and -triphosphatase activity, was used at 200 U/mL in ACSF. Brilliant Blue G (BBG, Sigma-Aldrich, no. B5133) was initially dissolved in nanopure water and further diluted in ACSF to a working concentration of 1 μM. In tissue slices, microglial

NIH-PA Author Manuscript

NIH-PA Author Manuscript

NIH-PA Author Manuscript

cell death events were identified by concomitant loss of GFP and gain of Sytox Orange (Eyo and Dailey, 2012). For all experimental conditions, we confirmed that the pH was at ~7.4 both before and after imaging.

For image processing, confocal images were collected and collated using Leica LAS AF software. Image stacks were assembled using Leica LAS AF software or ImageJ (Wayne Rasband, NIH). All images were processed using the "Smooth" filter (3 × 3 pixel array) in ImageJ to reduce noise. In all cases, comparisons were made on images processed identically. All movies generated represent the same z-tissue depth.

2.5. Whole-cell Patch Clamp Recording of Microglia in Neonatal Hippocampal Slices

Coronal brain slices (300 μm) were prepared from P4-P7 neonatal mice, as described previously (Wu et al., 2007). Hippocampal slices were transferred to a recovery chamber with oxygenated (95% O_2 and 5% CO_2) ACSF solution containing (in mM): NaCl, 124; $NaHCO_3$, 25; KCl, 2.5; KH_2PO_4, 1; $CaCl_2$, 2; $MgSO_4$, 2; glucose, 10; 300–310 mOsmol at room temperature. For divalent-free ACSF, both $CaCl_2$ and $MgSO_4$ were omitted and the osmolarity was adjusted with sucrose to 300–310 mOsmol. Brain slices were then transferred to a recording chamberand perfused with oxygenated ACSF at 3–4 ml/min at room temperature. All recordings were performed within 3 hours after mice were sacrificed. Recording pipette (5–6 MΩ) contained a K^+-based internal solution (K^+ IS) composed of (in mM): K-gluconate, 120; NaCl, 5; $MgCl_2$ 1; EGTA, 0.5; Mg-ATP, 2; Na_3GTP, 0.1; HEPES, 10; pH 7.2; 280–300 mOsmol. When using Cs^+-based internal solution (Cs^+ IS), K-gluconate was replaced by equimolar $CsMeSO_3$. The membrane potential was held at −60 mV throughout all experiments. Benzoyl-ATP (BzATP, Sigma-Aldrich, no. B6396) was used at 300 μM or 50 μM, and BBG was used at 5 μM to block BzATP-induced currents. Data were amplified and filtered at 2 kHz by a patch-clamp amplifier (Multiclamp 700B), digitalized (DIGIDATA 1440A), stored, and analyzed by pCLAMP (Molecular Devices, Union City, CA). Data were discarded when the input resistance changed >20 % during recording.

2.6. Microglial Cell Density Analysis

Microglia in hippocampal area CA1 were manually counted in confocal image stacks (15 images at 3 μm z-step size) obtained from heterozygous GFP-reporter mice. The volume of tissue sampled was calculated by measuring the 2D surface area of CA1 in ImageJ (Wayne Rasband, NIH) and multiplying this by the depth of the image stack (45 μm). The density of microglia was then calculated as: Number of microglia / Volume of tissue.

2.7. Statistical Analysis

For BV2 experiments, 5–7 experiments were performed for each condition. For confocal analysis in tissue slices, data from at least 28 slices and at least 3 animals were pooled and analyzed for each condition. All results are reported as mean ± standard deviation of the population. Statistical significance was assessed using Student's *t test.*

3. Results

3.1. OGD Induces BV2 Microglia Cell Death in a Calcium- and P2X7-dependent Manner

Oxygen and glucose deprivation (OGD) induces microglial cell death in rodent cell cultures (Lyons and Kettenmann, 1998; Yenari and Giffard, 2001). To determine the mechanisms involved in OGD-induced microglial cell death, we monitored the viability of BV2 microglia during OGD by time-lapse microscopy. BV2 cell death was evident as an initial cell blebbing or crenulation, followed by cell shrinkage and a persistent lack of movement (Fig. 1A and Movie 1). These features also correlated with uptake of a membrane-

NIH-PA Author Manuscript

NIH-PA Author Manuscript

NIH-PA Author Manuscript

impermeable fluorescent DNA-binding dye, Sytox, which labels nuclei of cells with compromised membranes but not living cells (Fig. 1B and Movie 2). Quantification showed that 6 hr of OGD significantly increased BV2 cell death from 4.94 ± 5.25% to 22.49 ± 8.01 % (Fig. 1C). Since calcium dysregulation can mediate glial-cell death (Alberdi et al., 2005), we investigated the role of calcium in OGD-induced BV2 cell death. Removal of calcium during OGD substantially reduced cell death to 2.94 ± 2.57 % (Fig. 1C). BV2 cells express ionotropic P2X7 receptors (Brautigam et al., 2005), which may facilitate calcium influx and induce cell death (Raouf et al., 2007). Indeed, we found that antagonism of P2X7Rs by Brilliant Blue G (BBG; 1 μM) significantly reduced OGD-induced BV2 cell death to 8.21 ± 6.21 % (Fig. 1C). These results indicate that calcium influx and P2X7R activation promote BV2 microglia cell death during OGD.

3.2. OGD Induces Calcium- and Purine-Dependent Microglial Cell Death in Neonatal Mouse Hippocampal Slices

Although we recently demonstrated that OGD induces microglial cell death in neonatal mouse brain tissue slices (Eyo and Dailey, 2012), the mechanisms of microglial cell death in tissues have not been studied previously. We quantified microglial cell death using dual-channel confocal time-lapse imaging in acute hippocampal slices from heterozygous $CX3CR1^{GFP/+}$ mice with GFP-expressing microglia in the presence of Sytox. Microglial cell death in slices was quantified by a concomitant loss of GFP and gain of Sytox during 6 hr of imaging, as described previously (Eyo and Dailey, 2012). Invariably, rapid loss of GFP was closely followed by gain of Sytox (or ToPro3) (Fig. 2 and Movie 3). This rapid loss of GFP signal is not due to photobleaching, which is a much slower event that happens concomitantly to all cells in the field of view. Only when these two events (loss of GFP and gain of Sytox) occurred together did we consider the microglial cell to have died.

Under control conditions, very few microglia die (0.05 ± 0.26 % of microglia; 30 slices; Fig. 3A, E). However, during OGD, microglial cell death was significantly increased (38.5 ± 11.6 % of microglia; 32 slices; Fig. 3B, E), although calcium omission prevented OGD-induced microglial cell death (0.9 ± 1.1 %; 31 slices; Fig. 3C, E and Movie 4). Analysis of fixed tissue slices 6 hr after treatment indicated that, in the absence of OGD, calcium-free medium itself did not alter the density of GFP+ microglial cells ($6.8 \pm 1.1 \times 10^{-6}$ microglia/μm^3; n = 9 slices) relative to control ($7.3 \pm 0.9 \times 10^{-6}$ microglia/μm^3; n = 8 slices; $P = 0.41$), consistent with there being very little baseline microglial cell death irrespective of the presence or absence of extracellular calcium.

Since OGD increases extracellular ATP ([ATP]e) in hippocampal slices (Juranyi et al., 1999; Frenguelli et al., 2007), and high [ATP]e can be cytotoxic to microglia (Ferrari et al., 1997), we speculated that degradation of [ATP]e would inhibit OGD-induced microglial cell death. Indeed, apyrase (200 U/mL), an ATP/ADP degrading enzyme, prevented OGD-induced microglial cell death (0.0005 ± 0.003 % of microglia; 26 slices; Fig. 3D, E). Together, these results indicate that OGD induces death of parenchymal microglia in neonatal slices through a calcium- and purine-dependent mechanism.

3.3. Expression of Functional P2X7R in Microglia in Neonatal Hippocampus

Although BV2 cells express P2X7Rs (Brautigam et al., 2005) and OGD-induced BV2 cell death was abolished by a P2X7R antagonist (Fig. 1), it is unknown whether parenchymal microglia in the neonatal hippocampus express *functional* P2X7Rs. Thus, we performed whole-cell patch clamp recordings in GFP-expressing microglia in the CA1 *stratum radiatum* (SR) of freshly isolated neonatal hippocampal slices (Fig. 4A). At a holding potential of −60 mV and normal K^+-based internal solution (IS), local puff application of a potent P2X7R agonist, benzoyl-ATP (BzATP, 300 μM, 1 s or 5 s), induced a rapid small

NIH-PA Author Manuscript

NIH-PA Author Manuscript

NIH-PA Author Manuscript

inward current followed by a substantial outward current (Fig. 4B). Consistent with our previous study (Wu et al., 2007), when intracellular K^+ was replaced by Cs^+, BzATP induced a small inward current but no outward current (Fig. 4B).

As expected for P2X7R currents, we found that BzATP (300 μM, 1 s) induced substantially larger inward currents (397.1 ± 68.2 pA, n = 6) when divalent cation-free ACSF was used. There was no significant increase in the BzATP current (402.6 ± 38.8 pA; n = 6) when the duration of puff application was increased to 5 s (Fig. 4B, E). Since the EC_{50} of BzATP at mouse P2X7Rs is ~80–100 μM (Hibbell et al., 2000; Donnelly-Roberts et al., 2009), we used lower concentrations of the agonist. BzATP at 50 μM induced smaller currents (104.8 ± 25.9 pA, n = 8, 1 s; 168.4 ± 19.7 pA, n = 8, 5 s) that were largely inhibited by BBG (Fig. 4C, E; n = 5). Voltage ramp test (from −120 mV to +100 mV, 200 ms) showed a reversal potential of the BzATP-induced inward currents at around 0 mV (n = 8). BBG (5 μM) inhibited the current but did not change its reversal potential (n = 5) (Fig. 4D). These results suggest that microglia express functional P2X7Rs in freshly prepared neonatal mouse hippocampal slices, as they do in adult mouse hippocampus (Avignone et al., 2008).

3.4. Pharmacological Modulation of P2X7R Alters OGD-Induced Microglial Cell Death in Neonatal Brain Slices

Having detected functional P2X7Rs in tissue microglia, we proceeded to test the hypothesis that P2X7Rs are involved in OGD-induced microglial cell death in brain tissues. To do this, we first employed a pharmacological approach. Application of BBG (1 μM) during OGD significantly reduced microglial cell death from 37.9 ± 11.4 % (n = 28 slices) to 26.3 ± 13.1 % (n = 28 slices; Fig. 5). Under non-OGD conditions, the density of GFP+ microglia was not significantly different between control slices ($6.8 \pm 1.1 \times 10^{-6}$ microglia/μm^3; n = 8 slices) and BBG-treated slices ($5.8 \pm 1.6 \times 10^{-6}$ microglia/μm^3; n = 8 slices; $P = 0.15$), indicating that BBG itself is not toxic and does not alter basal levels of microglial cell survival. These pharmacological data are consistent with the idea that P2X7R activation promotes OGD-induced microglial cell death.

3.5. Knockout of P2X7 Receptor Significantly Reduces OGD-Induced Microglial Cell Death

Since pharmacological reagents may not be entirely specific, we extended our studies with a genetic approach using P2X7R null mice. To visualize microglia, we crossed P2X7R null mice with GFP-reporter mice. There were no obvious differences in the morphology or distribution of microglia in hippocampal slices freshly isolated from P2X7R knockout (P2X7KO) and P2X7R heterozygous (P2X7Het) neonatal mice (Fig. 6A, B). Moreover, quantitative analyses of initial microglial density in hippocampal slices at the start of imaging showed no significant difference between P2X7RHet ($10.3 \pm 1.6 \times 10^{-6}$ microglia/μm^3; n = 17 slices; 3 mice) and P2X7RKO ($9.6 \pm 1.4 \times 10^{-6}$ microglia/μm^3; n = 19 slices; 3 mice) (Fig. 6C).

To directly compare OGD-induced microglial cell death in P2X7RKO and P2X7RHet tissues, hippocampal slices from littermate P2X7KO and P2X7Het neonatal mice were imaged simultaneously by multisite imaging. OGD-induced microglia cell death at 6 hr was extensive in all hippocampal areas in P2X7RHet slices (Fig. 6A') but not in the P2X7RKO slices (Fig. 6B'). Quantitative analyses (18 slices from 3 animals for each genotype) showed that microglial cell death was reduced to nearly half (57%) in the P2X7RKO (21.0 ± 11.8 %) relative to the P2X7RHet (36.4 ± 8.9 %) (Fig. 6D). Movie 5 shows a representative comparison of microglial cell death in P2X7RHet and P2X7RKO slices. Thus, genetic deletion of P2X7R protected tissue microglia from cell death during OGD. Taken together, our results using both pharmacological and genetic approaches demonstrate that P2X7Rs regulate OGD-induced microglial cell death in neonatal brain tissues.

NIH-PA Author Manuscript

NIH-PA Author Manuscript

NIH-PA Author Manuscript

4. Discussion

Our previous work using time-resolved imaging in live brain slices demonstrated that OGD rapidly inhibits microglial motility and induces microglial cell death (Eyo and Dailey, 2012). Here, we extend those findings to show that OGD-induced microglial cell death in cell culture and in tissue slices is dependent on extracellular calcium and is regulated by purinergic signaling. Our electrophysiological data demonstrate that microglia in acutely excised neonatal brain slices express functional P2X7 receptors, and both pharmacological and genetic approaches indicate that P2X7R activation contributes to OGD-induced microglial cell death. This is the first demonstration of a specific purinergic receptor regulating microglial cell survival in brain tissues. Given the mechanistic similarities in tissue slices and BV2 cell cultures, microglial cell death during OGD may occur cell autonomously *in situ* as it does in cell culture.

4.1. Neonatal Hippocampal Microglia Express Functional P2X7Rs

Previous studies have shown that cultured microglia express P2X7 receptors (Ferrari et al., 1996, 1997; Di Virgilio et. al., 1999). However, activation of microglia during the process of isolation and culturing may induce or upregulate receptor expression. Earlier work in brain slices from neonatal mouse white matter (Haas et al., 1996) and adult forebrain (Bouscein et al., 2003) support the idea that microglia express functional P2X7Rs in tissues. However, the identity of the receptor(s) mediating such currents was not definitively resolved because the agonists (ATP and BzATP) used in those studies may activate other P2 receptors (North, 2002), and neither study presented evidence for blockade of BzATP/ATP-induced currents by selective P2X7R antagonists. A more recent study showed BBG (3 μM)-sensitive, P2X7R–like currents in identified microglia in adult mouse hippocampal slices, and observed an increase in both P2X7 mRNA and BBG-sensitive currents in slices harvested 24 h but not 3 h after kainate-induced status epilepticus *in vivo* (Avignone et al., 2008). Here, we provide additional support for expression of functional P2X7Rs in microglia in the neonatal mouse hippocampus using a P2X7R agonist, BzATP (50 μM), to elicit current responses that are inhibited by a selective P2X7R antagonist, BBG (Fig. 4). These reagents are widely recognized to target P2X7Rs (Jiang et al., 2000; Friedle et al., 2010). A recent study of microglia in embryonic mouse spinal cord tissues likewise showed that high [ATP]e induces BBG-sensitive currents that are absent in P2X7R nulls (Rigato et al., 2012). Together, these data indicate that both embryonic and early postnatal microglia express functional P2X7Rs.

The normal physiological roles of the P2X7 receptor during neonatal development remain to be determined. P2X7 receptor signaling has been suggested to regulate phagocytosis (Gu et al., 2011) and microglial proliferation (Rigato et al., 2012). Although we have not tested the role of this receptor in microglial phagocytosis *in situ*, our observations in the early postnatal hippocampus failed to detect any difference in microglial cell density between P2X7R heterozygote and knockout littermates (Fig. 6C), suggesting that P2X7R does not contribute significantly to microglia colonization or proliferation during neonatal hippocampal development.

4.2. ATP- and P2X7R–dependent Cytotoxicity During Stroke

The function of P2X7R during brain ischemia has been controversial. Le Feuvre et al. (2003) reported similar infarct volumes in wild type and P2X7R null mice 24 hr after transient or permanent ischemia, suggesting that P2X7Rs are not primary mediators of neuronal cell death during early post-ischemic periods. However, more recent studies using selective pharmacological reagents have demonstrated that P2X7R inhibition protects oligodendrocytes (Domercq et al., 2010) and neurons (Arbeloa et al., 2012) *in vivo* when

NIH-PA Author Manuscript

NIH-PA Author Manuscript

NIH-PA Author Manuscript

assessed 3–7 d following ischemia. These studies indicate that P2X7R activation promotes death of oligodendrocytes and neurons after stroke *in vivo*. Our results here suggest that P2X7R activation also contributes to death of microglia. Although our study focuses on the first few hours during OGD and are most relevant to the early stages of ischemic injury, our data do not exclude the possibility that P2X7Rs also regulate activation of microglia and neuroinflammation at later post-ischemic stages (Yanagisawa et al., 2008; Chu et al., 2012). Given the evidence that microglia promote tissue repair following ischemia (Lalancette-Hebert et al., 2007; Narantuya et al., 2010; Faustino et al., 2011), our results imply that enhancing microglial survival during ischemia by antagonizing P2X7R activation could enhance tissue recovery after stroke.

4.3. Mechanisms of Microglial Cell Death During OGD

The mechanisms of P2X7-mediated microglial cell death during OGD have not been fully established but likely involve ATP-receptor activation and calcium influx within microglia. Previous studies have shown that extracellular ATP levels increase after OGD in hippocampal slices (Juranyi et al., 1999; Frenguelli et al., 2007) and during stroke *in vivo* (Melani et al., 2012). High [ATP]e can activate P2X7 receptors, resulting in increased membrane permeability to calcium and cell death (Ferrari et al., 1997; Raouf et al., 2007; Skaper, 2011). Our finding that OGD-induced death of BV2 cells in culture and parenchymal microglia in slices is dependent on extracellular calcium is consistent with P2X7R–mediated calcium influx. However, while OGD-induced cytotoxic calcium influx may occur via P2X7R channel opening or large pore formation, other calcium permeation pathways involving channel proteins such as pannexins also may be involved (Pelegrín, 2011).

Calcium removal during OGD virtually abolished death of both BV2 cells in culture and parenchymal microglia in acute brain slices. However, P2X7 receptors are only partial contributors to ischemic microglial cell death because, unlike calcium removal, both pharmacological inhibition (in cell culture and acute slices) and genetic deletion of P2X7 receptors did not completely protect microglia from ischemia-induced cell death (compare Fig. 3 with Figs. 5 and 6). This suggests involvement of other calcium-regulating mechanisms that remain to be identified.

OGD induced a P2X7R–dependent death of cultured BV2 cells in the absence of other cell types, suggesting an autocrine-based mechanism of ATP release and receptor activation. Because the mechanisms of OGD-induced cell death in dissociated cell culture and tissue slices appear similar, cell autonomous mechanisms may be sufficient to cause death of microglia *in situ*. However, in tissue settings, astrocytes and other cell types may contribute to ATP-mediated cell death. There is evidence that rodent astrocytes express P2X7R–like currents in cell culture (Duan et al., 2003; Nörenberg et al., 2010) and in brain slices (Oliveira et al., 2011), although another study using three different electrophysiological approaches failed to detect functional P2X7Rs on astrocytes in postnatal (P9–18) hippocampal slices using a similar concentration of BzATP (20 μM) to ours (50 μM) (Jabs et al., 2007). This latter study found that, unlike astrocytes, microglia in these slice preparations express functional P2X receptors, although the specific subtype(s) were not identified. Given our identification of functional P2X7Rs on microglia *in situ*, these data suggest that the cellular site of detrimental P2X7R activation in hippocampal slices during OGD is more likely microglia than astrocytes, further strengthening the case for cell autonomous mechanisms. However, at present we cannot rule out that, in tissue settings, a variety of cell types may contribute to ATP outflow leading to death of microglia.

NIH-PA Author Manuscript

NIH-PA Author Manuscript

NIH-PA Author Manuscript

4.4. Conclusion

In summary, using both pharmacological and genetic approaches, we provide evidence for calcium-dependent and P2X7R–mediated microglial cell death during OGD in brain tissues. Results from isolated cell culture studies suggest that OGD-induced microglial cell death may occur cell autonomously, and that P2X7R–dependent mechanisms operate (at least in part) within microglia. However, P2X7Rs are not the sole contributors to the purine- and calcium-dependent ischemic cell death, and other mechanisms remain to be discovered. Although future studies will have to be conducted to determine the relevance of these mechanisms to stroke *in vivo*, these results provide insights that may be directed towards developing therapies for recovery after stroke. Viewed more broadly, this is the first study to identify a purinergic receptor regulating microglial cell death in living brain tissues under *any* conditions and thus has significance for developing therapeutic strategies for protecting microglia at times when they may be beneficial, or potentially promoting microglial cell death when they are cytotoxic.

Supplementary Material

Refer to Web version on PubMed Central for supplementary material.

Acknowledgments

Supported by grants to M.E.D. from the American Heart Association (0950160G) and NIH (NS064006), and the Iowa Center for Molecular Auditory Neuroscience though NIH Grant P30 DC010362. We thank Ms. Leah Fuller for assistance with mouse colony management and genotyping, and Dr. Jonathan Doorn for gift of BV2 cells.

References

Alberdi E, Sanchez-Gomez MV, Matute C. Calcium and glial cell death. Cell Calcium. 2005; 38:417–425. [PubMed: 16095689]

Arbeloa J, Perez-Samartin A, Gottlieb M, Matute C. P2X7 receptor blockade prevents ATP excitotoxicity in neurons and reduces brain damage after ischemia. Neurobiol Dis. 2012; 45:954–961. [PubMed: 22186422]

Avignone E, Ulmann L, Levavasseur F, Rassendren F, Audinat E. Status epilepticus induces a particular microglial activation state characterized by enhanced purinergic signaling. J Neurosci. 2008; 28(37):9133–9144. [PubMed: 18784294]

Barreto G, White RE, Ouyang Y, Xu L, Giffard RG. Astrocytes: targets for neuroprotection in stroke. Cent Nerv Syst Agents Med Chem. 2011; 11:164–173. [PubMed: 21521168]

Boucsein C, Zacharias R, Farber K, Pavlovic S, Hanisch UK, Kettenmann H. Purinergic receptors on microglial cells: functional expression in acute brain slices and modulation of microglial activation in vitro. Eur J Neurosci. 2003; 17:2267–2276. [PubMed: 12814360]

Brautigam VM, Frasier C, Nikodemova M, Watters JJ. Purinergic receptor modulation of BV-2 microglial cell activity: potential involvement of p38 MAP kinase and CREB. J Neuroimmunol. 2005; 166:113–125. [PubMed: 15979729]

Burnstock G. Physiology and pathophysiology of purinergic neurotransmission. Physiol Rev. 2007; 87:659–797. [PubMed: 17429044]

Chu K, Yin B, Wang J, Peng G, Liang H, Xu Z, Du Y, Fang M, Xia Q, Benyan L. Inhibition of P2X7 receptor ameliorates transient global cerebral ischemia/reperfusion injury via modulating inflammatory responses in the rat hippocampus. J Neuroinflammation. 2012; 9:69. [PubMed: 22513224]

Di Virgilio F, Sanz JM, Chiozzi P, Falzoni S. The P2Z/P2X7 receptor of microglial cells: a novel immunomodulatory receptor. Prog Brain Res. 1999; 120:355–368. [PubMed: 10551011]

Domercq M, Perez-Samartin A, Aparicio D, Alberdi E, Pampliega O, Matute C. P2X7 receptors mediate ischemic damage to oligodendrocytes. Glia. 2010; 58:730–740. [PubMed: 20029962]

NIH-PA Author Manuscript

NIH-PA Author Manuscript

NIH-PA Author Manuscript

Donnelly-Roberts DL, Namovic MT, Han P, Jarvis MF. Mammalian P2X7 receptor pharmacology: comparison of recombinant mouse, rat and human P2X7 receptors. Br J Pharmacol. 2009; 157:1203–1214. [PubMed: 19558545]

Duan S, Anderson CM, Keung EC, Chen Y, Chen Y, Swanson RA. P2X7 receptor-mediated release of excitatory amino acids from astrocytes. J Neurosci. 2003; 23(4):1320–1328. [PubMed: 12598620]

Eyo U, Dailey ME. Effects of oxygen-glucose deprivation on microglial mobility and viability in developing mouse hippocampal tissues. Glia. 2012; 60:1747–1760. [PubMed: 22847985]

Faustino JV, Wang X, Johnson CE, Klibanov A, Derugin N, Wendland MF, Vexler ZS. Microglial cells contribute to endogenous brain defenses after acute neonatal focal stroke. J Neurosci. 2011; 31:12992–13001. [PubMed: 21900578]

Ferrari D, Chiozzi P, Falzoni S, Dal Susino M, Collo G, Buell G, Di Virgilio F. ATP-mediated cytotoxicity in microglial cells. Neuropharmacology. 1997; 36:1295–1301. [PubMed: 9364484]

Ferrari D, Los M, Bauer MK, Vandenabeele P, Wesselborg S, Schulze-Osthoff K. P2Z purinoreceptor ligation induces activation of caspases with distinct roles in apoptoticand necrotic alterations of cell death. FEBS Lett. 1999; 447:71–75. [PubMed: 10218585]

Ferrari D, Villalba M, Chiozzi P, Falzoni S, Ricciardi-Castagnoli P, Di Virgilio F. Mouse microglial cells express a plasma membrane pore gated by extracellular ATP. J Immunol. 1996; 156:1531–1539. [PubMed: 8568257]

Frenguelli BG, Wigmore G, Llaudet E, Dale N. Temporal and mechanistic dissociation of ATP and adenosine release during ischaemia in the mammalian hippocampus. J Neurochem. 2007; 101:1400–1413. [PubMed: 17459147]

Friedle SA, Curet MA, Watters JJ. Recent patents on novel P2X(7) receptor antagonists and their potential for reducing central nervous system inflammation. Recent Pat CNS Drug Discov. 2010; 5:35–45. [PubMed: 19705995]

Ginsberg M. Neuroprotection for ischemic stroke: Past, present and future. Neuropharmacology. 2008; 55:363–389. [PubMed: 18308347]

Gu BJ, Saunders BM, Petrou S, Wiley JS. P2X(7) is a scavenger receptor for apoptotic cells in the absence of its ligand, extracellular ATP. J Immunol. 2011; 187:2365–2375. [PubMed: 21821797]

Haas S, Brockhaus J, Verkhratsky A, Kettenmann H. ATP-induced membrane currents in ameboid microglia acutely isolated from mouse brain slices. Neuroscience. 1996; 75:257–261. [PubMed: 8923539]

Hanley PJ, Kronlage M, Kirschning C, Del Rey A, Di Virgilio F, Leipziger J, Chessell IP, Sargin S, Filippov MA, Lindemann O, Mohr S, Konigs V, Schillers H, Bahler M, Schwab A. Transient P2X7 receptor activation triggers macrophage death independent of Toll-like receptors 2 and 4, caspase-1, and pannexin-1 proteins. J Biol Chem. 2012; 287:10650–10663. [PubMed: 22235111]

Hayashi Y, Tomimatsu Y, Suzuki H, Yamada J, Wu Z, Yao H, Kagamiishi Y, Tateishi N, Sawada M, Nakanishi H. The intra-arterial injection of microglia protects hippocampal CA1 neurons against global ischemia-induced functional deficits in rats. Neuroscience. 2006; 142:87–96. [PubMed: 16844302]

Hibell AD, Kidd EJ, Chessell IP, Humphrey PP, Michel AD. Apparent species differences in the kinetic properties of P2X(7) receptors. Br J Pharmacol. 2000; 130:167–173. [PubMed: 10781013]

Imai F, Suzuki H, Oda J, Ninomiya T, Ono K, Sano H, Sawada M. Neuroprotective effect of exogenous microglia in global brain ischemia. J Cereb Blood Flow Metab. 2007; 27:488–500. [PubMed: 16820801]

Jabs R, Matthias K, Grote A, Grauer M, Seifert G, Steinhauser C. Lack of P2X receptor mediated currents in astrocytes and GluR type glial cells of the hippocampal CA1 region. Glia. 2007; 55:1648–1655. [PubMed: 17849469]

Jeong HK, Ji KM, Kim B, Kim J, Jou I, Joe EH. Inflammatory responses are not sufficient to cause delayed neuronal death in ATP-induced acute brain injury. PLoS One. 2010; 5:e13756. [PubMed: 21060796]

Jiang LH, Mackenzie AB, North RA, Surprenant A. Brilliant blue G selectively blocks ATP-gated rat P2X(7) receptors. Mol Pharmacol. 2000; 58:82–88. [PubMed: 10860929]

NIH-PA Author Manuscript

NIH-PA Author Manuscript

NIH-PA Author Manuscript

Jung S, Aliberti J, Graemmel P, Sunshine MJ, Kreutzberg GW, Sher A, Littman DR. Analysis of fractalkine receptor CX(3)CR1 function by targeted deletion and green fluorescent protein reporter gene insertion. Mol Cell Biol. 2000; 20:4106–4114. [PubMed: 10805752]

Juranyi Z, Sperlagh B, Vizi ES. Involvement of P2 purinoceptors and the nitric oxide pathway in [3H]purine outflow evoked by short-term hypoxia and hypoglycemia in rat hippocampal slices. Brain Res. 1999; 823:183–190. [PubMed: 10095025]

Kitamura Y, Takata K, Inden M, Tsuchiya D, Yanagisawa D, Nakata J, Taniguchi T. Intracerebroventricular injection of microglia protects against focal brain ischemia. J Pharmacol Sci. 2004; 94:203–206. [PubMed: 14978360]

Kitamura Y, Yanagisawa D, Inden M, Takata K, Tsuchiya D, Kawasaki T, Taniguchi T, Shimohama S. Recovery of focal brain ischemia-induced behavioral dysfunction by intracerebroventricular injection of microglia. J Pharmacol Sci. 2005; 97:289–293. [PubMed: 15684564]

Lalancette-Hebert M, Gowing G, Simard A, Weng YC, Kriz J. Selective ablation of proliferating microglial cells exacerbates ischemic injury in the brain. J Neurosci. 2007; 27:2596–2605. [PubMed: 17344397]

Le Feuvre RA, Brough D, Touzani O, Rothwell NJ. Role of P2X7 receptors in ischemic and excitotoxic brain injury in vivo. J Cereb Blood Flow Metab. 2003; 23:381–384. [PubMed: 12621313]

Liu HT, Sabirov RZ, Okada Y. Oxygen-glucose deprivation induces ATP release via maxi-anion channels in astrocytes. Purinergic Signal. 2008; 4:147–154. [PubMed: 18368522]

Lyons SA, Kettenmann H. Oligodendrocytes and microglia are selectively vulnerable to combined hypoxia and hypoglycemia injury in vitro. J Cereb Blood Flow Metab. 1998; 18:521–530. [PubMed: 9591844]

Matute C, Domercq M, Sanchez-Gomez MV. Glutamate-mediated glial injury: mechanisms and clinical importance. Glia. 2006; 53:212–224. [PubMed: 16206168]

Melani A, Corti F, Stephan H, Muller CE, Donati C, Bruni P, Vannucchi MG, Pedata F. Ecto-ATPase inhibition: ATP and adenosine release under physiological and ischemic in vivo conditions in the rat striatum. Exp Neurol. 2012; 233:193–204. [PubMed: 22001157]

Melani A, Turchi D, Vannucchi MG, Cipriani S, Gianfriddo M, Pedata F. ATP extracellular concentrations are increased in the rat striatum during in vivo ischemia. Neurochem Int. 2005; 47:442–448. [PubMed: 16029911]

Narantuya D, Nagai A, Sheikh AM, Masuda J, Kobayashi S, Yamaguchi S, Kim SU. Human microglia transplanted in rat focal ischemia brain induce neuroprotection and behavioral improvement. PLoS One. 2010; 5:e11746. [PubMed: 20668522]

Nedergaard M, Dirnagl U. Role of glial cells in cerebral ischemia. Glia. 2005; 50:281–286. [PubMed: 15846807]

Nelson KB. Perinatal ischemic stroke. Stroke. 2007; 38:742–745. [PubMed: 17261729]

Neumann J, Gunzer M, Gutzeit HO, Ullrich O, Reymann KG, Dinkel K. Microglia provide neuroprotection after ischemia. FASEB J. 2006; 20:714–716. [PubMed: 16473887]

Nörenberg W, Schunk J, Fischer W, Sobottka H, Riedel T, Oliveira JF, Franke H, Illes P. Electrophysiological classification of P2X7 receptors in rat cultured neocortical astroglia. Br J Pharmacol. Aug; 2010 160(8):1941–1952. [PubMed: 20649592]

North RA. Molecular physiology of P2X receptors. Physiol Rev. 2002; 82:1013–1067. [PubMed: 12270951]

Oliveira JF, Riedel T, Leichsenring A, Heine C, Franke H, Krügel U, Nörenberg W, Illes P. Rodent cortical astroglia express in situ functional P2X7 receptors sensing pathologically high ATP concentrations. Cereb Cortex. Apr; 2011 21(4):806–820. [PubMed: 20739479]

Pelegrín P. Many ways to dilate the P2X7 receptor pore. British J Pharm. 2011; 163:908–911.

Raouf R, Chabot-Dore AJ, Ase AR, Blais D, Seguela P. Differential regulation of microglial P2×4 and P2X7 ATP receptors following LPS-induced activation. Neuropharmacology. 2007; 53:496–504. [PubMed: 17675190]

Rigato C, Swinnen N, Buckinx R, Couillin I, Mangin JM, Rigo JM, Legendre P, Le Corronc H. Microglia proliferation is controlled by P2X7 receptors in a Pannexin-1-independent manner

NIH-PA Author Manuscript

NIH-PA Author Manuscript

NIH-PA Author Manuscript

during early embryonic spinal cord invasion. J Neurosci. 2012; 32:11559–11573. [PubMed: 22915101]

Ryu JK, Kim J, Choi SH, Oh YJ, Lee YB, Kim SU, Jin BK. ATP-induced in vivo neurotoxicity in the rat striatum via P2 receptors. Neuroreport. 2002; 13:1611–1615. [PubMed: 12352612]

Skaper SD. Ion channels on microglia: therapeutic targets for neuroprotection. CNS Neurol Disord Drug Targets. 2011; 10:44–56. [PubMed: 21143139]

Solle M, Labasi J, Perregaux DG, Stam E, Petrushova N, Koller BH, Griffiths RJ, Gabel CA. Altered cytokine production in mice lacking P2X(7) receptors. J Biol Chem. 2001; 276:125–132. [PubMed: 11016935]

Szydlowska K, Tymianski M. Calcium, ischemia and excitotoxicity. Cell Calcium. 2010; 47:122–129. [PubMed: 20167368]

Takano T, Oberheim N, Cotrina ML, Nedergaard M. Astrocytes and ischemic injury. Stroke. 2009; 40:S8–S12. [PubMed: 19064795]

Weinstein JR, Koerner IP, Moller T. Microglia in ischemic brain injury. Future Neurol. 2010; 5(2): 227–246. [PubMed: 20401171]

Wu LJ, Vadakkan KI, Zhuo M. ATP-induced chemotaxis of microglial processes requires P2Y receptor-activated initiation of outward potassium currents. Glia. 2007; 55:810–821. [PubMed: 17357150]

Wu LJ, Wu G, Sharif MRA, Baker A, Jia Y, Fahey FH, Luo HR, Feener EP, Clapham DE. The voltage-gated proton channel Hv1 enhances brain damage from ischemic stroke. Nat Neurosci. 2012; 15:565–573. [PubMed: 22388960]

Yanagisawa D, Kitamura Y, Takata K, Hide I, Nakata Y, Taniguchi T. Possible involvement of P2X7 receptor activation in microglial neuroprotection against focal cerebral ischemia in rats. Biol Pharm Bull. 2008; 31(6):1121–1130. [PubMed: 18520042]

Yenari MA, Giffard RG. Ischemic vulnerability of primary murine microglial cultures. Neurosci Lett. 2001; 298:5–8. [PubMed: 11154822]

Yrjanheikki J, Keinanen R, Pellikka M, Hokfelt T, Koistinaho J. Tetracyclines inhibit microglial activation and are neuroprotective in global brain ischemia. Proc Natl Acad Sci USA. 1998; 95:15769–15774. [PubMed: 9861045]

NIH-PA Author Manuscript

NIH-PA Author Manuscript

NIH-PA Author Manuscript

Highlights for Eyo et al

- Oxygen-glucose deprivation (OGD) induces calcium-dependent microglial cell death.
- OGD-induced microglial cell death is regulated by extracellular purines.
- Neonatal microglia *in situ* express P2X7 receptor-like currents.
- Disruption of P2X7 receptors significantly reduces OGD-induced death of microglia.

NIH-PA Author Manuscript
NIH-PA Author Manuscript
NIH-PA Author Manuscript

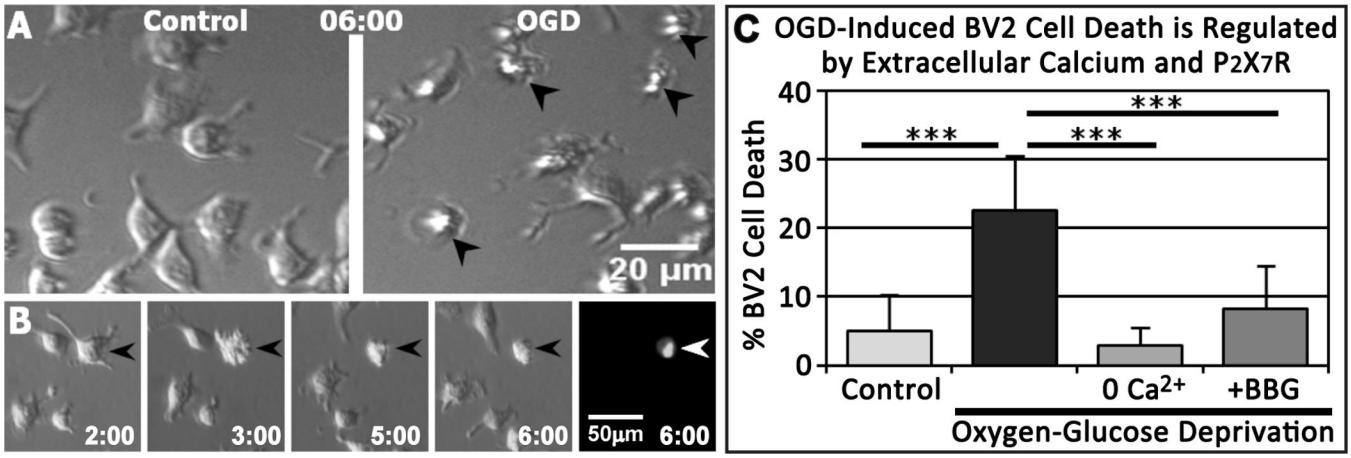

Figure 1.

OGD-Induced BV2 Cell Death is Regulated by Extracellular Calcium and P2X7R Signaling. **A**, BV2 cells were imaged by modified Hoffmann modulation contrast for 6 hr under control conditions (**left**) or OGD (**right**). OGD-induced cell death was identified by abrupt morphological changes, including blebbing or cell crenulation, followed by lack of movement (dead cells identified by arrowheads in **right panel**). **B**, Selected images from a time-lapse sequence showing that only blebbing/crenulating cells label with a fluorescent DNA-binding dye, Sytox, a marker of cell death (arrowheads). Time shown in hr:min after start of OGD. **C**, OGD increased BV2 cell death, but the removal of extracellular calcium or application of 1 µM BBG significantly inhibited OGD-induced cell death. n = 5–7 experiments per condition. ***P < 0.005 relative to OGD.

NIH-PA Author Manuscript

NIH-PA Author Manuscript

NIH-PA Author Manuscript

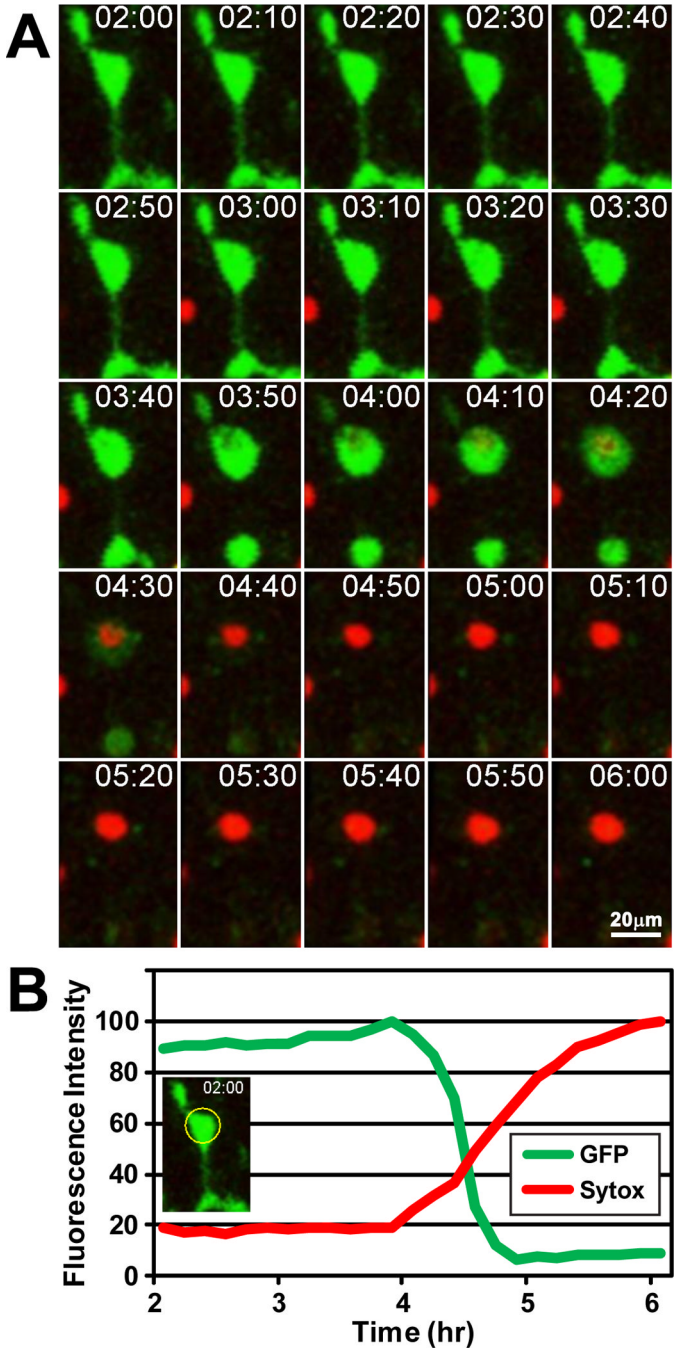

Figure 2.

Time-lapse imaging shows changes in fluorescence labeling of microglia during OGD-induced cell death. **A**, Montage of images from a time-lapse experiment in a tissue slice showing OGD-induced microglial cell death evident as a rapid loss of GFP and gain of Sytox (between 4:10 and 4:30). The first image corresponds to 2 h after start of OGD. Time is shown in h:min. A time-lapse sequence of these images is available as Movie 3. **B**, Quantification of fluorescence intensity (normalized to 100%) showing concomitant loss of GFP and gain of Sytox in the cell body area (yellow circle) of the dying microglial cell.

NIH-PA Author Manuscript

NIH-PA Author Manuscript

NIH-PA Author Manuscript

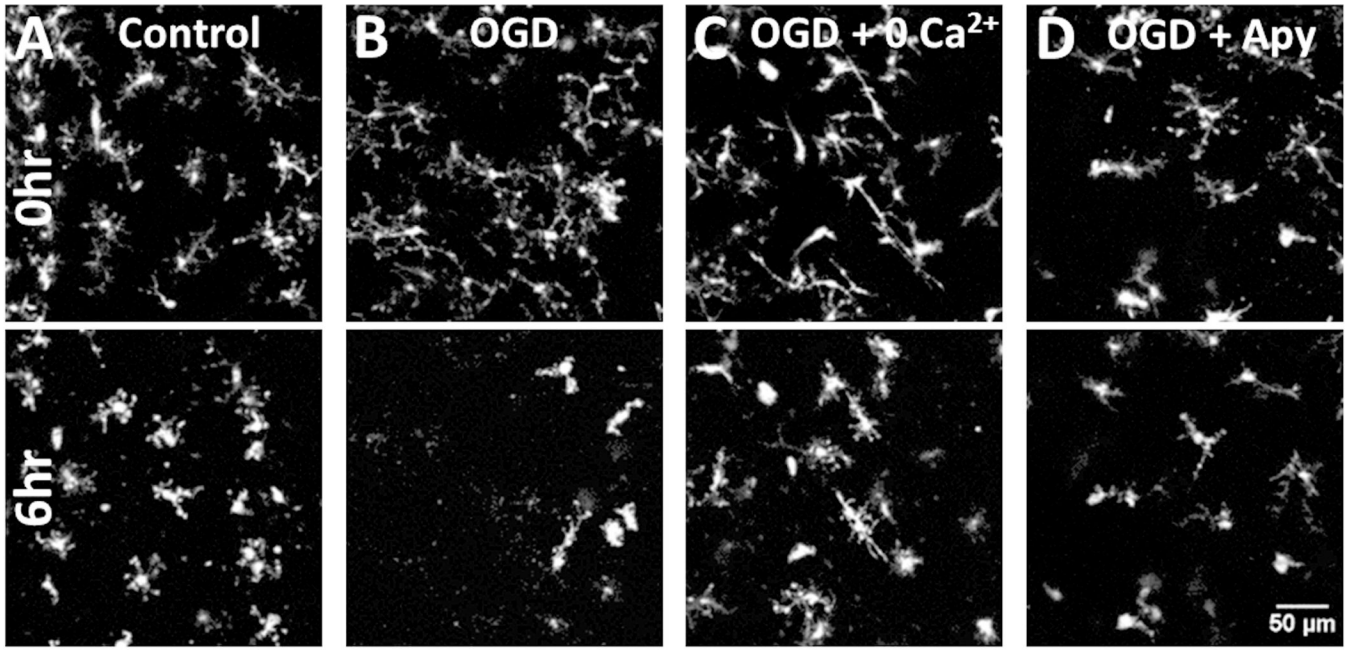

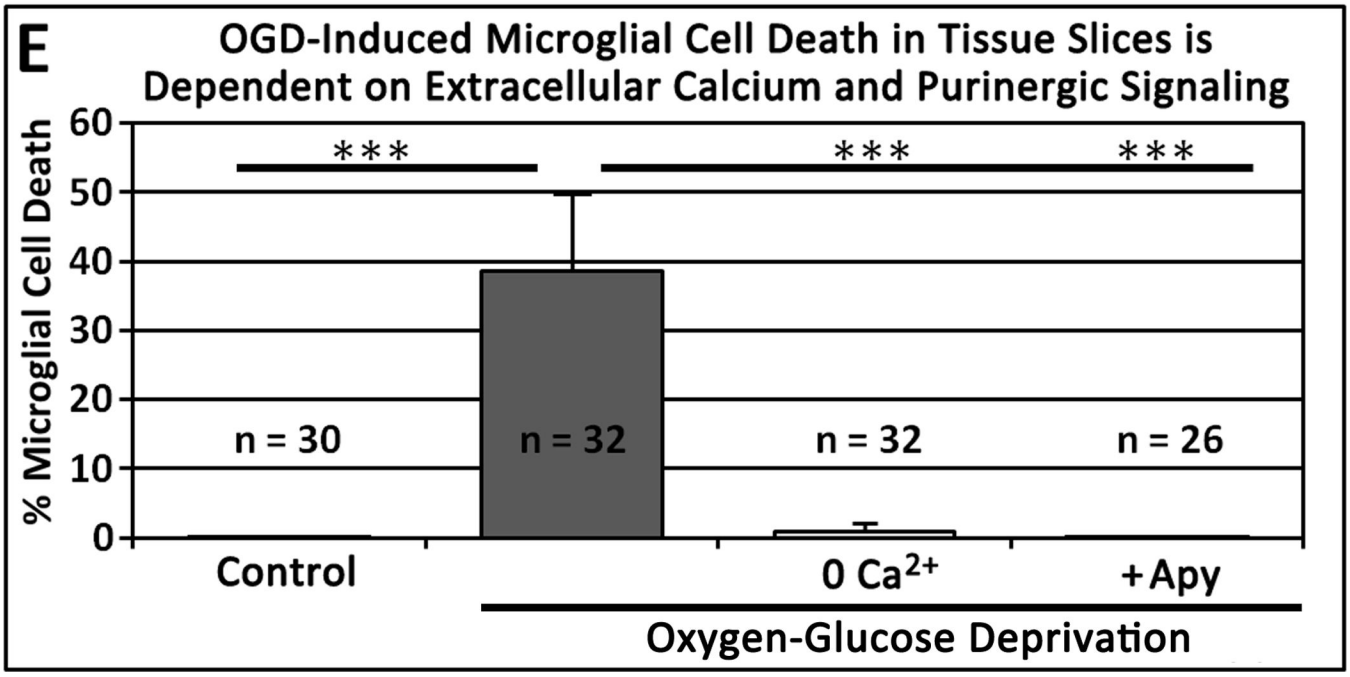

Figure 3.

OGD-Induced Microglial Cell Death in Tissue Slices is Dependent on Extracellular Calcium and Purinergic Signaling. **A–D**: Representative images of hippocampal slices containing GFP-expressing microglia at the beginning (**top**) and end (**bottom**) of a 6 hr imaging session under the following conditions: control (**A**); OGD (**B**); OGD without calcium (**C**); and OGD with 200 U/mL apyrase (**D**). **E**, Quantitative analysis shows a significant increase in microglial cell death during OGD that is abolished by removal of extracellular calcium or application of apyrase. ***P < 0.005 relative to OGD.

NIH-PA Author Manuscript
NIH-PA Author Manuscript
NIH-PA Author Manuscript

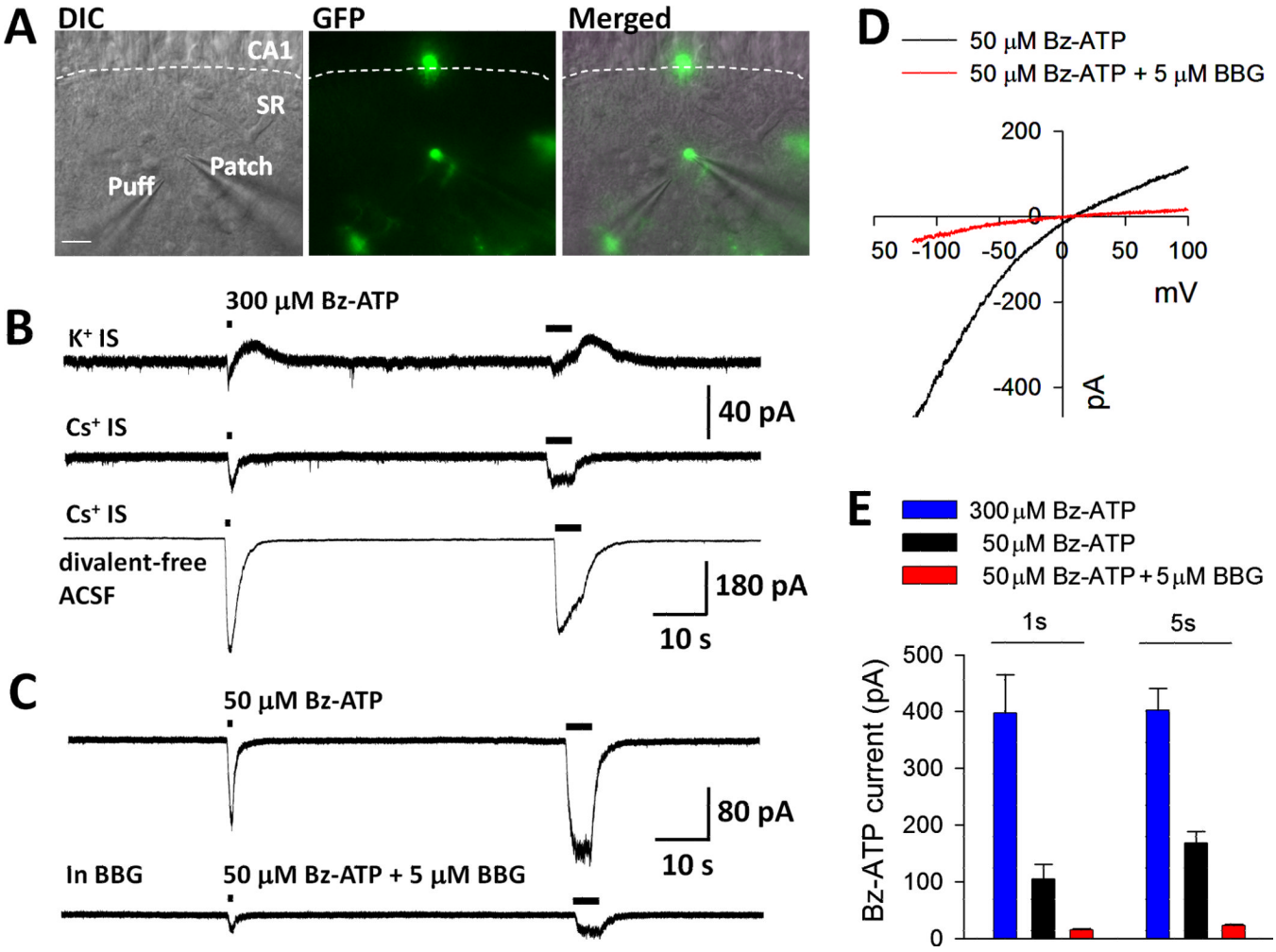

Figure 4.

Microglia Express Functional P2X7R in Acute Neonatal Mouse Hippocampal Slices. **A**, Representative images showing whole-cell patch-clamp recording and drug application through puffer pipette in hippocampal CA1 *stratum radiatum (SR)* microglia. The dashed line shows the boundary of CA1 *stratum pyramidale* (CA1) and *SR* layers in the hippocampus. GFP-expressing microglia appear green. Scale bar: 20 μm. **B**, Using K^+ based internal solution (IS), local application of BzATP (300 μM, 1 s and 5 s) induced a rapid inward current followed by an outward current (n = 5). Outward currents were eliminated in Cs^+-based IS (n = 4). BzATP inward currents were significantly potentiated in divalent cation-free conditions. Holding potential was −60 mV. **C**, Representative traces showing that BBG (5 μM) inhibits BzATP (50 μM, 1 s or 5 s) induced currents (n = 5). **D**, Voltage ramp tests (from −120 mV to +100 mV, 200 ms) were used to assess the reversal potential of the BzATP (50 μM)-induced currents with or without BBG. **E**, Summarized results show the concentration dependent BzATP currents (1 s and 5 s application) and their inhibition by BBG.

NIH-PA Author Manuscript

NIH-PA Author Manuscript

NIH-PA Author Manuscript

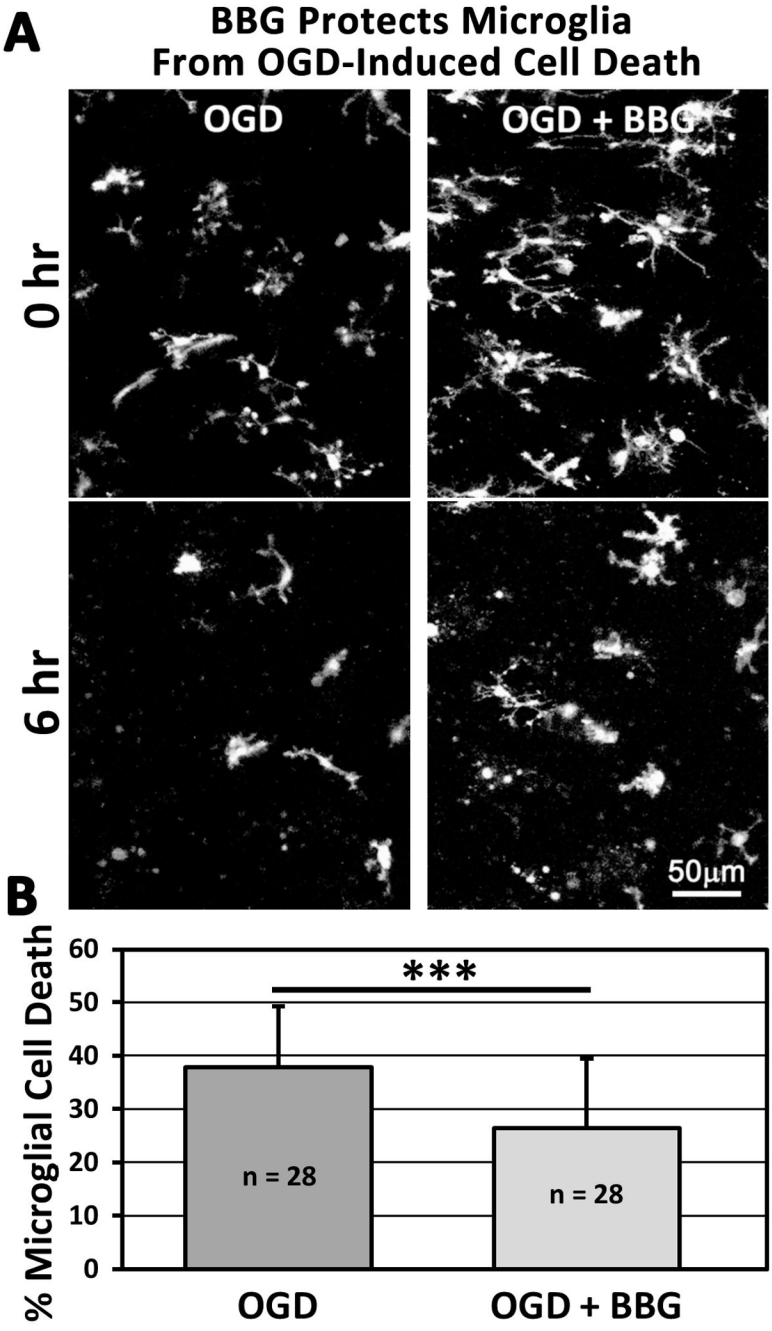

Figure 5.

Pharmacological Inhibition of P2X7R Activation with BBG Protects Microglia from OGD-Induced Cell Death. **A**, Representative images of hippocampal slices containing GFP-expressing microglia at the beginning (**top**) and end (**bottom**) of a 6 hr imaging session under OGD conditions in the absence (**left)** or presence (r**ight**) of a P2X7R antagonist (BBG; 1 μM). **B**, OGD- induced microglial cell death in tissue slices is significantly inhibited by P2X7R antagonist. ***P < 0.005.

NIH-PA Author Manuscript
NIH-PA Author Manuscript
NIH-PA Author Manuscript

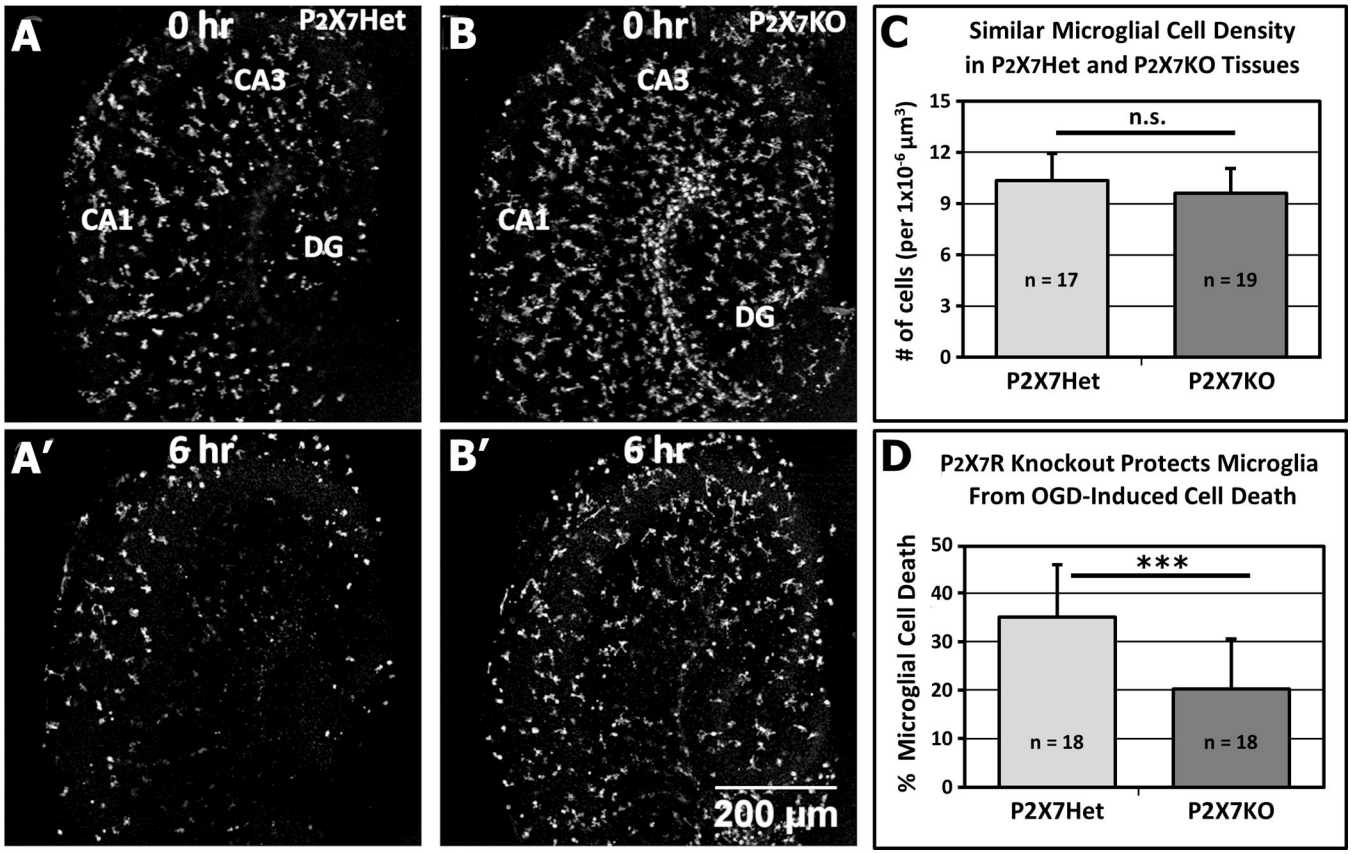

Figure 6.

Knockout of P2X7R Reduces OGD-Induced Microglial Cell Death. **A–B**', Representative slices from P2X7RHet ($P2X7R^{+/-}$:$CX3CR1^{GFP/+}$; **A, A**') and P2X7RKO ($P2X7R^{-/-}$:$CX3CR1^{GFP/+}$; **B, B**') neonatal mice subjected to OGD and imaged simultaneously. At the start of time-lapse imaging, microglia are present throughout all hippocampal areas in both P2X7RHet and P2X7RKO tissues (**A, B**), and microglial density is not significantly different (**C**). By 6 hours of OGD (**A**', **B**'), microglia are markedly reduced in number in the P2X7RHet slice (**A**'), but many microglia persist in the P2X7RKO slice (**B**'). **D**, Quantitative analysis shows that OGD-induced microglia cell death is reduced to nearly half (57%) in P2X7RKO slices relative to P2X7RHet. ***P < 0.005.